

Characterization of Amide–Alkanediol Intermolecular Interactions

Rafael Alcalde,[†] Gregorio García,[†] José Luis Trenzado,^{*,‡} Mert Atilhan,[§] and Santiago Aparicio^{*,†}

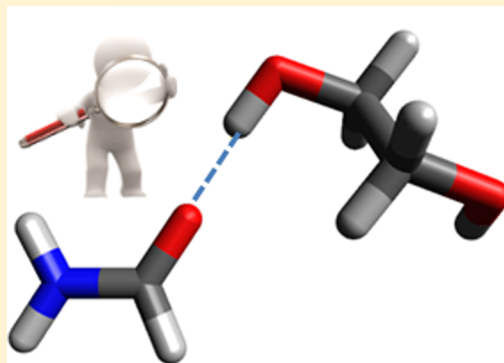
[†]Department of Chemistry, University of Burgos, 09001 Burgos, Spain

[‡]Departamento de Física, Universidad de Las Palmas de Gran Canaria, 35017 Las Palmas G.C., Spain

[§]Department of Chemical Engineering, Qatar University, P.O. Box 2713, Doha, Qatar

S Supporting Information

ABSTRACT: The properties of formamide + 1,2-alkanediol binary liquid systems were studied both at the macro- and microscopic levels using a combined experimental and computational methodology. Physicochemical properties, infrared spectroscopy, and solvatochromic studies together with classic molecular dynamics and quantum chemistry calculations allowed the main characteristics of these binary fluids to be inferred with regard to the variations of hydrogen bonding with formamide and 1,2-alkanediol molecular structures, mixture composition, and temperature. The complexity of these liquid systems arising from the presence of three different functional groups, which may act as hydrogen bond donors and acceptors, is analyzed, allowing a detailed picture to be inferred of the studied systems which is of relevance both for basic liquid state theory and for industrial purposes.



INTRODUCTION

The understanding of mechanisms and physicochemical models relating intermolecular forces with macroscopic properties in the liquid state is of pivotal relevance for basic science purposes,^{1,2} for the development of statistical thermodynamic models able to describe properly the liquid state main features,³ but also for applied and industrial applications, for developing materials in the liquid phase suitable for the required technologies.⁴ Due to the complexity of the liquid state physical chemistry,⁵ it is necessary to carry out systematic studies on the effects of functional groups on the development of intermolecular interactions⁶ and their effects on liquid phase structuring from a nanoscopic viewpoint for complex liquids.^{7,8} Likewise, this understanding would allow reliable structure–property relationships to be developed for predicting purposes,⁹ and thus, a rational design of solvents, liquid extracting agents, gas absorbents, and materials for related applications.¹⁰

Amides are key molecules because of containing the carbonyl and amino functional groups in the same molecular unit (peptide bond), which is of pivotal relevance for biochemical purposes as models for describing intermolecular interactions in proteins or nucleic acids.^{11–14} Likewise, amides are used as solvents^{15,16} in many industrial applications such as extraction,¹⁷ and gas separation,^{18,19} and thus, the knowledge of the macro- and nanoscopic properties of amide-based fluid is of great relevance. Formamide (FOR) is the simplest amide molecule, almost ubiquitous in the universe,²⁰ and thus, it has been used to model and study the behavior of amides in the liquid phase with regard to the role of intermolecular interactions developing the hydrogen bonding network between the amino and carbonyl groups, which controls the

structure and properties of the liquid phase.^{12,21} Available studies have allowed inferring the main structural features in liquid formamide. Bakó et al.²² summarized the main conclusions obtained from the literature analysis with regard to FOR intermolecular forces in the liquid phase, showing the discrepancies for the different studies in the characteristics of the hydrogen bonding networks. FOR is able to develop cyclic dimers and also chainlike aggregations by H-bonding; the population of cyclic dimmers varies from 3.0 to 12.0% in the different available studies,²² although a value close to 8% seems to be confirmed by some experimental measurements.²¹ The inclusion of alkyl chains in the $-\text{NH}_2$ group leads to remarkable changes in the hydrogen bonding ability of formamides, and thus, the two simplest derived molecules *N*-methylformamide (NMF) and *N,N*-dimethylformamide (DMF) have also been the subject of remarkable research.^{14,23} The hydrogen bonded network in pure FOR is characterized by the formation of two H-bonds per molecule on average,^{14,24} whereas the structure of DMF is characterized by intermolecular interactions through dipole–dipole mechanisms.^{23,25} Likewise, considering the presence of both donor and acceptor hydrogen bonding groups in FOR and NMF, or only acceptor in DMF, the behavior of these molecules upon mixing with other relevant hydrogen bond donors and/or acceptors has also been studied^{14,26–28} In particular, formamides + alcohols have been studied because of the relevance of having $-\text{OH}$, $-\text{NH}_2$, and $-\text{COH}$ functional groups in the same fluid with regard to

Received: January 29, 2015

Revised: March 12, 2015

Published: March 12, 2015

the characterization of hydrogen bonding in complex fluids.^{29–32} The complex structuring in formamide + alcohol binary liquid mixtures rising from the H-bonding and its changes with mixture composition should be even more complicated when considering alkanediols, in which the presence of two hydroxyl groups may lead to interactions with the available groups in the formamides developing H-bonded networks. To our knowledge, no previous studies were reported in the literature for formamides + 1,2-alkanediols, and thus, considering the relevant features of 1,2-alkanediols,^{33–35} and the complexity of H-bonding in these liquid mixtures, the study of these systems deserves detailed attention. Therefore, the structure and properties of formamide (FOR, NMF, or DMF) + 1,2-alkanediol (1,2-ethanediol, ED; 1,2-propanediol, PD; or 1,2-butanediol, BD), Figure 1, liquid mixtures was studied in this work.

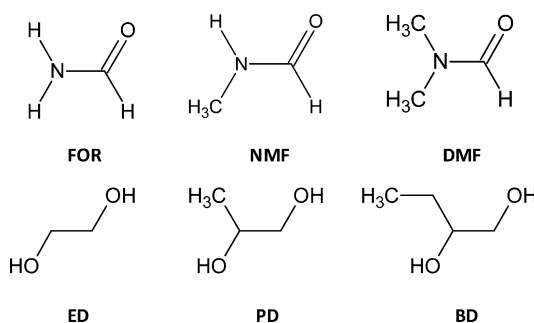


Figure 1. Molecular structures of compounds studied in this work.

The characterization of properties for formamide + 1,2-alkanediol liquid mixtures developed in this work combines an experimental and computational approach as a function of mixture composition and temperature. Physicochemical properties were measured to infer deviations from thermodynamic ideality and their relationships with changes in H-bonding characteristics and strength. These intermolecular interactions were also analyzed through infrared spectroscopy studies, which through the deconvolution of relevant amide peaks allowed the evolution of H-bonds to be inferred. Fluid polarity was measured through solvatochromic studies. Then, characterization of intermolecular interactions at the molecular level was done through a quantum chemical approach, using density functional theory (DFT) methods, for the analysis of short-range interactions, combined with classic molecular dynamics simulations (MD). This approach allowed a detailed picture of the H-bonding in the studied liquid mixtures and its relationship with macroscopic physicochemical properties to be obtained, providing information about the role of the involved functional groups in the liquid structuring.

METHODS

Chemicals. Amide and 1,2-alkanediol samples used for the thermophysical and spectroscopic studies were obtained from commercial suppliers (Table S1, Supporting Information). Fluids were dried using molecular sieves, and they were degassed with ultrasound. No further purification was considered. The reliability of the used samples and experimental procedures was assessed through the comparison of physicochemical properties obtained in this work with previous literature studies (Table S1, Supporting Information). Binary mixtures in the whole composition range for amide

(FOR, NMF, or DMF) + 1,2-alkanediol (ED, PD, or BD) binary systems were prepared by mass (Mettler AE240 balance, ± 0.0001 g), with ± 0.00004 uncertainty in mole fraction (x).

Thermophysical Measurements. Density (ρ) and viscosity (η) were measured for the amide + 1,2-alkanediol binary systems at atmospheric pressure and as a function of mixture composition and temperature (283.15–313.15 K range). The experimental procedures for ρ and η measurements used in this work were previously described,³⁶ and thus, it would be described briefly in this work. ρ was measured to $\pm 2 \times 10^{-5}$ g cm⁻³, with $\pm 1 \times 10^{-2}$ K temperature uncertainty, with an Anton Paar DMA 60/602 oscillating U-tube densimeter. Viscosity was measured with 0.2% average uncertainty, for $\pm 1 \times 10^{-2}$ K temperature uncertainty, with a Schott-Geräte CT1450/2 viscometer. Excess molar volume, V^E , and mixing viscosity, $\Delta\eta$, were calculated from the known relationships.³⁷

Spectroscopic Measurements. Attenuated total reflection infrared (ATR-IR) studies were carried out using a Smart Thermal ARK device (zinc selenide crystal) in a Nicolet Nexus spectrometer, with the temperature controlled to 293.15 ± 1 K. Solvatochromic measurements were carried out for Reichardt's dye (2,6-diphenyl-4-(2,4,6-triphenyl-1-pyridinio)phenolate; Aldrich, 95% purity) using a Shimadzu UV-1603 spectrophotometer with the cell temperature controlled to 293.15 ± 0.1 K. Samples for solvatochromic measurements were prepared by dilution of the dye in the corresponding fluid to 1×10^{-4} M. The normalized Reichardt's parameter, E_T^N , was calculated from the wavenumbers corresponding to the maxima in spectral curves as previously defined.^{38,39}

DFT Calculations. The main objective of these simulations was to carry out a potential energy surface (PES) analysis for the intermolecular interactions in formamide + 1,2-alkanediol mixtures. Such a conformational landscape would allow obtaining information on the preferred relative disposition between molecules as a function of the mixture composition. For this purpose, several formamide + 1,2-alkanediol 1: n and n :1 ($n = 1, 4$) clusters were optimized. These calculations were carried out using the Becke gradient corrected exchange functional⁴⁰ and Lee–Yang–Parr correlation functional⁴¹ with three parameters (B3LYP)⁴² method, along with the 6-311+G** basis set. Optimized minima were checked through their vibration frequencies. For those simulations wherein two or more molecules are present, different starting points were employed in order to study different initial arrangements, paying attention to the disposition of minimal energy. Binding energies, ΔE , were calculated as the difference among the pair energy and the sum of corresponding optimized monomer energies at the same theoretical level, with the basis set superposition error (BSSE) corrected through the counterpoise procedure.⁴³ DFT calculations were done using the Gaussian 09 (revision D.01) package.⁴⁴

Molecular Dynamics Simulations. This study was carried out with the MDynaMix v.5.2 package.⁴⁵ As starting points of each simulation, cubic boxes containing 500 total molecules (density ~ 0.3 g cm⁻³) were built with the Packmol program.⁴⁶ All of the simulations were carried out in the NPT ensemble considering periodic boundary conditions. The Nosé–Hoover method was used for the control of pressure and temperature along the simulations. The Ewald summation method,⁴⁷ with a cutoff radius of 15 Å, was applied for Coulombic interaction. The equations of motion were solved by using the Tuckerman–Berne double time step algorithm,⁴⁸ with 1 and 0.1 fs long and short time steps, respectively. Lennard-Jones terms

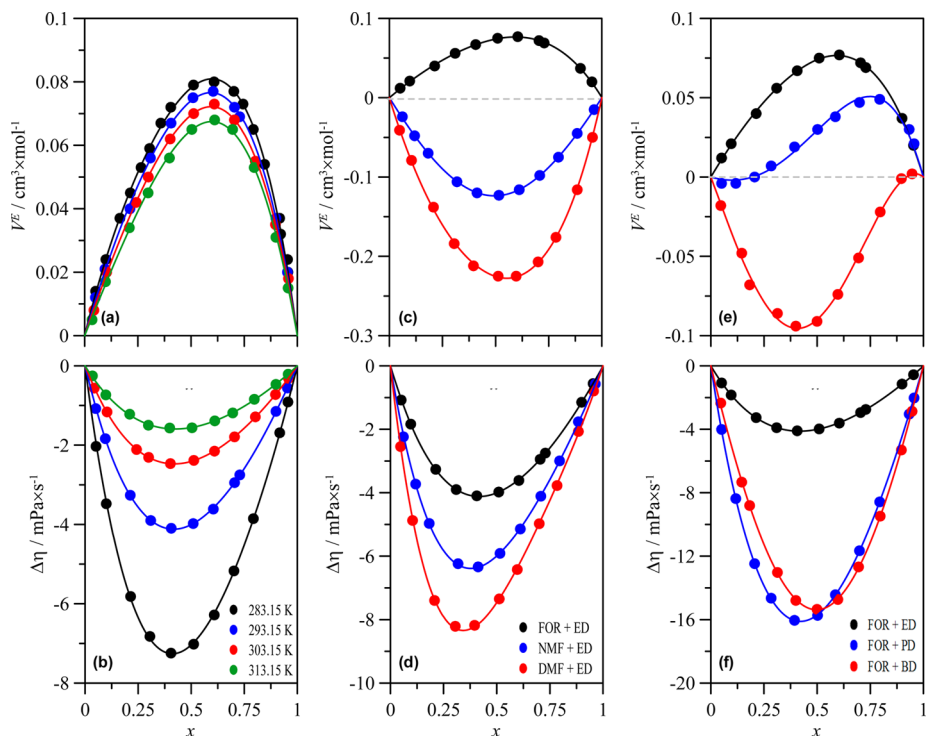


Figure 2. Excess molar volume, V^E , and mixing viscosity, $\Delta\eta$, for (a, b) x FOR + $(1 - x)$ ED as a function of temperature, (c, d) x formamides + $(1 - x)$ ED as a function of amide type, and (e, f) x FOR + $(1 - x)$ 1,2-alkanediol as a function of alkanediol type. x stands for amide mole fraction. Symbols show experimental data and lines fits to Redlich–Kister polynomials. All values at 293.15 K.

were handled according to Lorentz–Berthelot mixing rules. The simulations were carried out in two steps: (i) initial equilibration periods for 1 ns, assured through constancy of potential energy, followed by (ii) 10 ns production runs.

Force field parametrizations used are reported in Table S2 (Supporting Information). Atomic charges used in the simulations were obtained with the ChelpG⁴⁹ method for optimized structures as considered in the DFT Calculations section.

Several sets of simulations were arranged to infer the most relevant nanoscopic features in the studied systems. First, simulations on pure amides and 1,2-alkanediols were done for force field validation purposes and for the analysis of the most relevant features in pure fluids that will change upon mixing. Second, the composition effect on mixture properties was analyzed with simulations for the FOR + ED system as a function of mole fraction, at 293 K. Third, the effect of the type of amide was studied with simulations for amide + ED, and vice versa, and the effect of 1,2-alkanediol by analyzing FOR + 1,2-alkanediol, all of them at equimolar compositions and 293 K. Fourth, the effect of temperature was studied in the 283–313 K range (10 K steps) for FOR + ED, FOR + BD, and DMF + ED for equimolar mixtures.

RESULTS AND DISCUSSION

Thermophysical Characterization. Experimental density and viscosity data for formamides (FOR, NMF, or DMF) + alkanediols (ED, PD, or BD) for the 283.15–313.15 K range are reported in Tables S3, S4, and S5 (Supporting Information), and derived excess and mixing properties (V^E and $\Delta\eta$) are plotted in Figure 2. FOR + ED liquid mixtures are highly nonideal and characterized by expansion upon mixing, Figure 2a, with maxima in excess volume at 0.62 FOR mole

fraction (roughly 1:2 molar ratio). Likewise, although the V^E maximum decreases with increasing temperature (19% on going from 293.15 to 313.15 K), the mole fractions for these maxima do not change. These results show weakening of intermolecular interactions upon mixing rising from the disruption of FOR–FOR and ED–ED strong hydrogen bondings, which are not totally balanced by the creation of new FOR–ED interactions. This effect is particularly important for FOR rich regions, as the maxima in V^E skewed toward FOR rich mixtures shows, although the disruption effect of the second type of molecule is important for both FOR and ED interactions. The disruptive effect upon mixing FOR and ED is confirmed by the very large negative $\Delta\eta$ shown in Figure 2b, with the minima appearing at roughly 0.4 FOR mole fraction. In contrast with V^E , $\Delta\eta$ minima appear at roughly 0.4 FOR mole fraction, and this composition for the maxima does not change with increasing temperature. This may be justified considering that the viscosity of pure ED is roughly 5 times larger than that for pure FOR (Table S1, Supporting Information), and thus, although the expansive behavior is larger in the case of FOR rich mixtures, the effects on viscosity are larger for ED rich mixtures considering the large viscosity of these fluids.

The effect of the amide type on excess and mixing properties may be inferred from the results reported in Figure 2c,d for formamides (FOR, NMF, or DMF) + ED at 293.15 K. The results in Figure 2c show that whereas the system FOR + ED leads to positive V^E (expansion upon mixing) both NMF + ED and DMF + ED lead to negative V^E (contraction upon mixing), with larger negative V^E for DMF containing systems. Likewise, although all the considered formamide + ED systems show negative $\Delta\eta$ in the whole composition range at 293.15 K, they increase in absolute value on going from FOR to NMF to

DMF. This behavior shows that upon methylation of the $-\text{NH}_2$ group the ability of formamide molecules to develop self-association through hydrogen bonding decreases (and it is absent in the case of DMF), and thus, strong heteroassociations with ED molecules are developed in contrast with the less associated states in pure amides, which leads to contraction upon mixing and very large mixing viscosity. Likewise, the minima for $\Delta\eta$, Figure 2d, shift toward larger ED mole fractions with increasing $-\text{NH}_2$ methylation, which shows the relevance of hydrogen bonding between formamides and ED molecules and their disruptive effects on the ED self-association, especially for DMF, which may act only as a hydrogen bond acceptor.

The changes in physicochemical properties with the type of 1,2-alkanediol are reported in Figure 2e,f. In the case of FOR + alkanediol (ED, PD, or BD), the systems evolve from expansive behavior for FOR + ED or + PD to contractive for FOR + BD, and at the same time, $\Delta\eta$ is roughly 4 times larger for those systems containing PD and BD than for ED. The two hydroxyl groups are placed in positions 1 and 2 of the alkylic chains, and thus, the main difference between the studied alkanediols is the increasing alkyl chain, which leads to less efficient molecular packing, as shown by the decreasing densities on going from pure ED to PD to BD (Table S1, Supporting Information). These larger alkylic chains also increase the viscosity of pure alkanediols, but the larger change is produced on going from ED to PD, whereas changes on going from pure PD to BD are lower (Table S1, Supporting Information). Therefore, for a fixed type of amide (FOR in Figure 2e,f), there is a remarkable steric effect that should justify the negative excess molar volume for those systems containing large alkylic chains (DMF) because of the presence of void spaces in pure alkanediol that are rearranged upon mixing and would be able to fit small FOR molecules, which at the same time could develop heteroassociations through hydrogen bonding between amide and alkanediol functional groups. In the case of $\Delta\eta$, the very large values for FOR + PD and FOR + BD are very similar for both systems, in agreement with the close values of viscosity data for both pure alkanediols, which points to the disruptive effect of FOR molecules on the alkanediol structuring through the hydrophobic alkylic chains leading to a large decrease in viscosity.

Spectroscopic Characterization. The ATR-IR spectra were recorded for formamides (FOR, NMF, or DMF) + alkanediol (ED, PD, or BD) at 293.15 K, although a detailed analysis is only reported for FOR + ED as a function of composition in Figures 3–5. Amides have three well-known main bands in the IR spectral range (named the amide I, II, and III bands), whereas the most useful IR feature in alcohols is the OH stretching band, and thus, these IR spectral properties can be used to analyze intermolecular interactions. Nevertheless, the IR spectral regions corresponding to N—H and O—H stretching vibrations overlap in the same frequency range (3000 – 3300 cm^{-1}), and thus, it was not possible to separate through peak deconvolution those features corresponding to each functional group. Therefore, the IR analysis of intermolecular interactions in FOR + ED liquid mixtures was carried out for the 1500 – 1700 cm^{-1} region corresponding to C=O stretching (amide I band) and $-\text{NH}_2$ bending (amide II band) which is a well-defined region without overlapping with any alkanediol peaks. Figure 3a shows the changes in ATR-IR spectra as a function of composition. The results show a narrow and well-defined peak corresponding to C=O stretching combined with a shoulder at lower frequencies corresponding

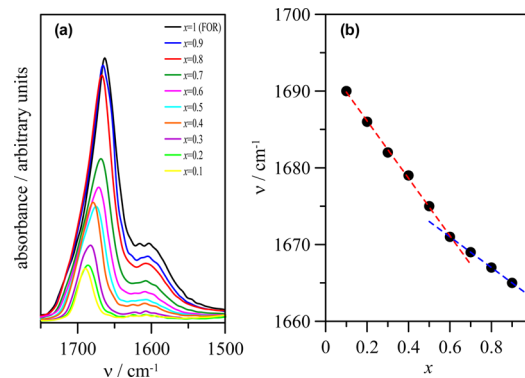


Figure 3. (a) ATR-IR spectra in the amide I band region and (b) wavenumber, ν , for the maxima of the amide I band for x FOR + $(1 - x)$ ED at 293 K. x stands for FOR mole fraction.

to the NH_2 bending peak. The CO stretching peak decreases in intensity with increasing ED mole fraction, and at the same time, the peaks are blueshifted, Figure 3b. Nevertheless, this blueshifting with increasing ED mole fraction does not follow a linear trend, and two well-defined regions are obtained for compositions up to 0.6 FOR mole fraction and for larger concentrations. These results show the development of FOR–ED hydrogen bonding through the CO site, and whereas for x (FOR mole fraction) > 0.6 most of the CO sites are hydrogen bonded to FOR molecules, for $x < 0.6$, most of them are hydrogen bonded to hydroxyl groups in ED molecules. This behavior can be quantified more in detail if a peak deconvolution is carried out as explained in Figure 4

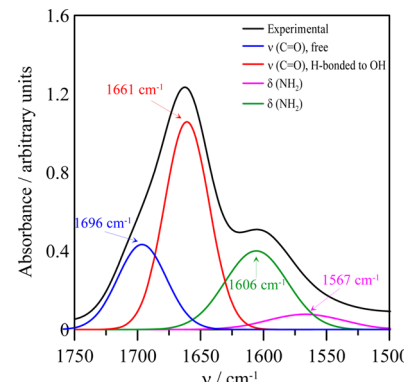


Figure 4. Deconvolution of the ATR-IR spectrum, using Gaussian curves, of pure FOR in the amide I region, with deconvoluted peaks assigned to the stretching vibration of free C=O (not H-bonded), H-bonded to hydrogen atoms in OH, and to NH_2 bending modes, $\delta(\text{NH}_2)$.

considering that the 1500 – 1700 cm^{-1} spectral region can be split in four peaks assigned to free and H-bonded CO and NH_2 groups. It should be remarked that considering a CO group as free does not mean that this molecule is a monomer because it may have the CO free group but it may be H-bonded through the NH_2 group. The maxima of the peaks assigned to CO stretching vibrations follow a non-linear trend for both free and H-bonded groups clearly separated by 0.6 FOR mole fraction, Figure 5a. Likewise, the percentage of non-hydrogen-bonded CO groups follows a complex pattern with FOR dilution in ED, Figure 5b. For x in the 0.6 to pure FOR range, the percentage of free CO groups is 31–34%, with a poorly defined maximum,

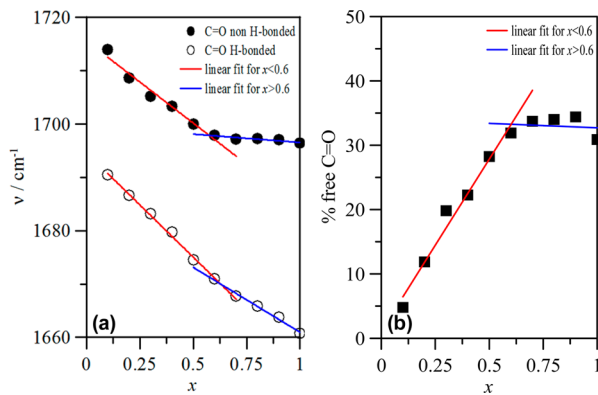


Figure 5. Results of ATR-IR spectra deconvolution, using Gaussian curves, for x FOR + $(1-x)$ ED at 293 K. Panel a shows wavenumbers for the maxima of peaks assigned to the stretching of C=O free (non-H-bonded) and H-bonded (both to H_2N and HO). Panel b shows the percentage of free C=O calculated from the ratio of the area corresponding to the C=O free peak to the total area corresponding to C=O stretching vibrations (free + H-bonded). x stands for FOR mole fraction.

but for $x < 0.6$, this percentage decreases in a steep and linear way, reaching a percentage around 5% for very diluted mixtures of FOR in ED. Therefore, most of the FOR molecules are H-bonded to hydroxyl groups in ED, whereas the percentage of free CO groups in amide rich regions is much larger, which would justify the very large changes in mixing viscosity reported in Figure 2. Hence, ATR-IR results confirm the presence of two well-defined mixing regions for FOR + ED mixtures defined as mixtures with prevailing homoassociations between amide molecules ($x > 0.6$) and those systems ($x < 0.6$) in which FOR molecules are mainly H-bonded to hydroxyl groups.

The solvatochromic measurements carried out in this work allow the polarity of the mixtures and the changes with mole fraction and thus with intermolecular hydrogen bonding to be characterized. The solvatochromic results for all the formamide + alkanediol systems are reported in Table S6 (Supporting Information), and the main results are summarized in Figure 6. In the case of FOR + ED, Figure 6a, the liquid mixture follows a nonlinear trend with positive deviations and a maximum at 0.4 FOR mole fraction, which is in agreement with the properties reported in previous sections. This points to an

increase of polarity for FOR + ED mixtures as a consequence of heteroassociations between FOR and ED molecules. Analogous behavior is obtained for FOR + PD, whereas in the case of FOR + BD deviations from linearity are smaller as a consequence of the larger alkyl chains in alkanediol, which decrease the polarity of mixtures, Figure 6a. Likewise, the effect of amide type is reported in Figure 6b, which also shows positive deviations from linearity for the three studied amides with ED. In the case of DMF + ED mixtures, a sudden change in mixture polarity is obtained for DMF mole fractions larger than 0.9, which is a consequence of the absence of H-bonding in pure DMF and the low number of H-bonds for mixtures with high DMF concentration.

Density Functional Theory Study of Short Range Interactions

In this work, DFT simulations were used to carry out an analysis of the PES for formamide + alkanediol clusters with different compositions. Thus, we obtained information on the preferred relative disposition between involved molecules and the effect of the composition on calculated binding energies. The experimental results reported in previous sections have shown that intermolecular H-bonds between formamides and alkanediols are the main short-range interaction in this kind of mixtures. Therefore, binding energies as a function of the composition for the optimized cluster at the DFT level were used for estimating the interaction strength. The structure and binding energies for all the studied formamide (FOR, NMF, or DMF) + alkanediol (ED, PD, or BD) clusters are reported in Figures S1–S14 (Supporting Information), whereas the main results are summarized in Figures 7–9.

The optimized geometries for 1:1 clusters along with their corresponding binding energies are reported in Figure 7. DFT results confirm that the main interaction (H-bond) between formamides and 1,2-alkanediols is carried out through O (C=O) and H (hydroxyl) atoms, whose lengths are around 1.84 Å. Calculated binding energies are not significantly affected by the type of formamide or 1,2-alkanediol molecules. For formamide + 1,2-alkanediol 1:1 clusters, $|\Delta E|$ are in the 30.80 kJ·mol⁻¹ (NMF + PD) to 24.81 kJ·mol⁻¹ (FOR + ED) range, except for DMF + ED clusters with $|\Delta E| = 14.01$ kJ·mol⁻¹. Binding energies follow the same trends despite the selected 1:1 cluster. In the case of FOR + 1,2-alkanediol, $|\Delta E| \approx 4.00$ kJ·mol⁻¹ upon chain elongation up to PD, while this increase is slightly lower (≈ 2.59 kJ·mol⁻¹) to BD. As a function of the type of formamide, *N*-methyl substitution leads to an increase of 0.91 kJ·mol⁻¹, while dimethyl functionalization yields some lower binding energies than those for FOR + 1,2-alkanediol. This effect is larger for DMF + ED, whose $|\Delta E|$ diminishes up to 14.01 kJ·mol⁻¹. For NMF + 1,2-alkanediol 1:1 clusters, two different geometries were optimized as a function of the rotational angle through the N—C bond. Thus, Figure 7 shows those geometries wherein the methyl group is in the *trans*-configuration with respect to the O atom. However, isoenergetical structures are obtained when the methyl group is in the *cis*-configuration.

The effect of the composition on binding energies was studied through the optimization of clusters with different molecular ratios. Figure 8 displays binding energies for formamide + ED 1: n clusters and their corresponding optimized geometries for FOR + ED clusters (detailed results for all 1: n clusters may be found in the Supporting Information). For 1:2 and 1:3 clusters, different arrangements (labeled as a, b, and c) were optimized. Two conformers were found for NMF + 1,2-alkanediols as a

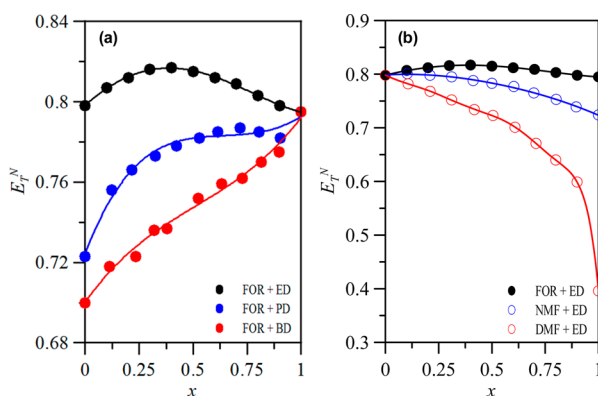


Figure 6. Normalized Reichardt's parameter, E_T^N , for (a) x FOR + $(1-x)$ 1,2-alkanediol (ED, PD, or BD) and (b) x formamides (FOR, NMF, or DMF) + $(1-x)$ ED at 293.15 K. x stands for formamide mole fraction.

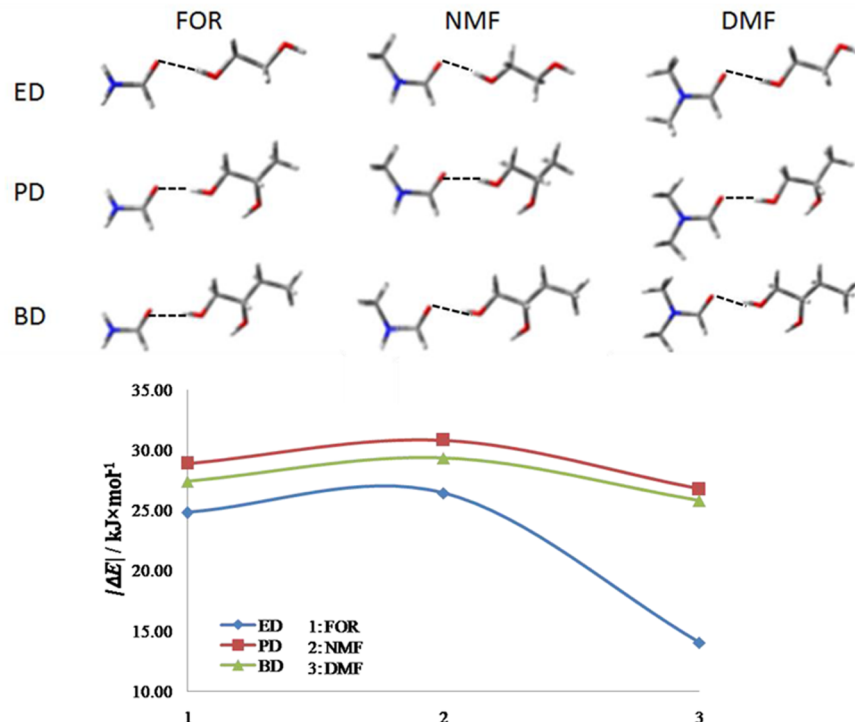


Figure 7. Optimized geometry for formamide (FOR, NMF, or DMF) + alkanediol (ED, PD, or BD) 1:1 clusters at the B3LYP/6-311+G** theoretical level (top) along with their binding energies, ΔE (bottom).

function of the rotational angle through the N–C bond. However, for clusters 1: n ($n > 1$), both conformations of NMF (labeled as trans or cis) do not yield the same binding energy. Lower $|\Delta E|$ are also obtained for FOR + ED, as for 1:1 clusters. The following discussion on DFT results is mainly focused on FOR + ED systems, although similar qualitative conclusions are obtained for the remaining systems. Considering the optimized FOR geometry, four different formamide positions able to interact with 1,2-alkanediols could be defined, i.e., O and H from the amide moiety (O1 and H2) and both H (H1) from the $-\text{NH}_2$ motif. For 1:2 clusters, considering the three different arrangements, FOR interacts with the first ED through O1, as previously described for 1:1 clusters. In arrangement 1:2a/1:2c, the FOR molecule establishes a H-bond (through H1) with the O (hydroxyl) atom. Both arrangements 1:2a and 1:2c yield similar $|\Delta E| \approx 48.45 \text{ kJ} \cdot \text{mol}^{-1}$. However, for 1:2b, whose $|\Delta E| = 60.11 \text{ kJ} \cdot \text{mol}^{-1}$, the second ED molecule is linked to the first ED through a H-bond between their OH groups. This larger $|\Delta E|$ value points out that ED + ED interactions are stronger than FOR + ED ones (through $-\text{NH}_2$ and hydroxyl motifs). The 1:3 clusters could be defined as the sum of different 1:2 clusters, wherein O1 positions are always occupied in the same way as in 1:1 clusters. $|\Delta E|$ values for 1:3 clusters follow the order 1:3a < 1:3b < 1:3c. The structure 1:3a could be considered as the sum of 1:2a and 1:2c clusters, with all the donor–acceptor sites in FOR being fully occupied by ED molecules. Arrangement 1:3b could be defined as a sum of 1:2a + 1:2b clusters, wherein the central FOR only interacts with two ED molecules, while the third ED is only interacting with another ED. Arrangement 1:3c would be similar to 1:2c; however, one ED is simultaneously linked to both FOR (through H1) and ED (through their OH groups). This interaction is only possible for FOR + 1,2-alkanediol mixtures. However, methyl substitution hinders this amide–1,2-alkane-

diol (H1–O) H-bond. Hence, such an ED molecule is only interacting with another ED. Again, $|\Delta E|$ values point out that ED + ED interactions are stronger than FOR + ED ones. Finally, the 1:4 cluster could be defined as the sum of 1:3a + 1:3c ones. The 1:4 cluster provides the largest $|\Delta E|$ values, mainly due to ED–ED interactions. In short, despite the cluster composition, the central amide molecule is only able to form intermolecular bonds with two 1,2-alkanediol molecules (see the 1:2a cluster). Likewise, ED molecules are forced to interact with other ED molecules, except for FOR + 1,2-alkanediols wherein for $n = 3$ there is also a weak formamide + 1,2-alkanediol interaction through H1. On the basis of such results, we could expect that some macroscopic properties related to H-bonds would be unaffected (or slightly affected) for ED molar fraction larger than 0.66.

Figure 9 gathers results regarding FOR + ED n :1 clusters (see the Supporting Information for more detailed information for all formamide + 1,2-alkanediol n :1 clusters). The ED molecule only presents two regions (OH groups) to interact with FOR. The intermolecular H-bond carried out through this position is similar to those described for 1:1 clusters; i.e., H (hydroxyl in ED)/O (FOR) plays as a H-bond donor/acceptor. For FOR + ED n :1 clusters with $n = 1$, both H (OH groups) are forming H-bonds with amides. Moreover, FOR molecules are interacting with both central ED and FOR molecules: (i) with the first one, there is a trough and H-bond between the O (ED) and H2 (FOR, linked to the C=O group); (ii) with the latter, there is a H-bond between both amide groups. On the basis of optimized geometries for FOR + ED n :1 clusters, we could conclude that (within the composition range studied through DFT simulations) 1,2-alkanediols are able to interact with up to four amide molecules. In addition, for amide molar fractions larger than 0.75, there are also amide + amide intermolecular interactions.

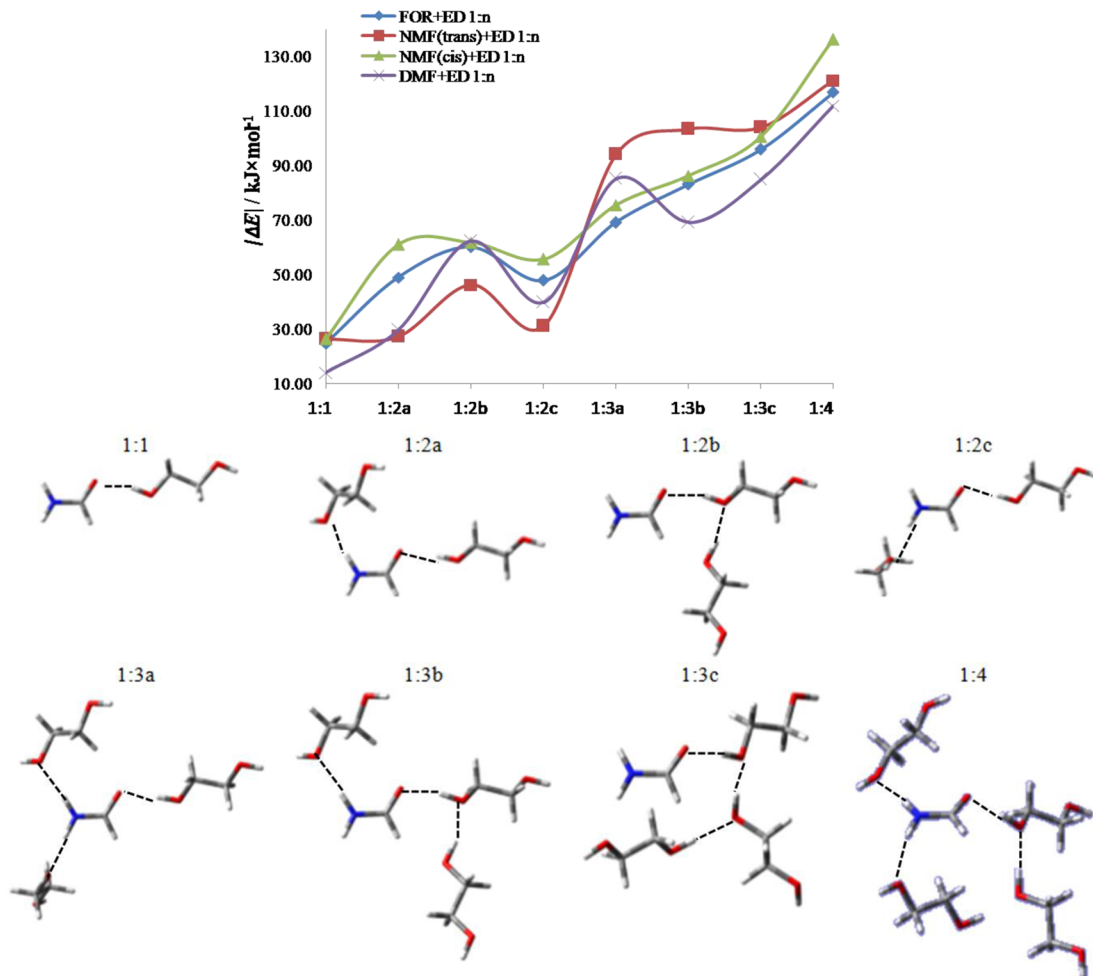


Figure 8. Binding energies, ΔE , for formamide (FOR, NMF, or DMF) + ED 1: n clusters (top) and optimized geometries for FOR + ED 1: n clusters (bottom). All calculated at the B3LYP/6-311+G** level.

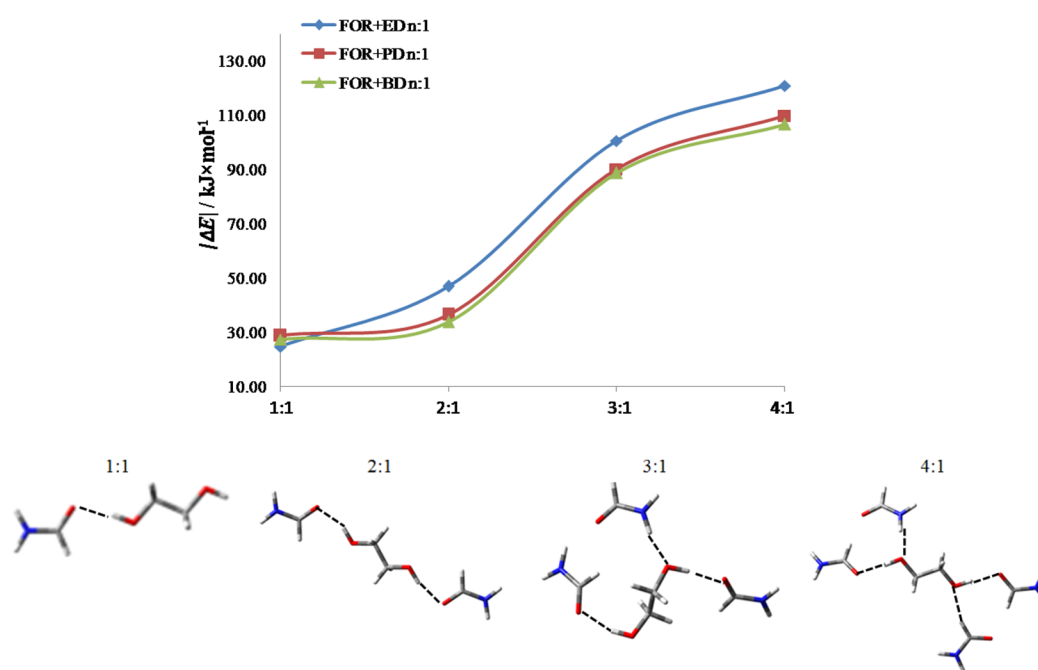


Figure 9. Calculated binding energies for FOR + alkanediol (ED, PD, or BD) $n:1$ clusters (top) and optimized geometries for FOR + ED $n:1$ clusters (bottom). All calculated at the B3LYP/6-311+G** level.

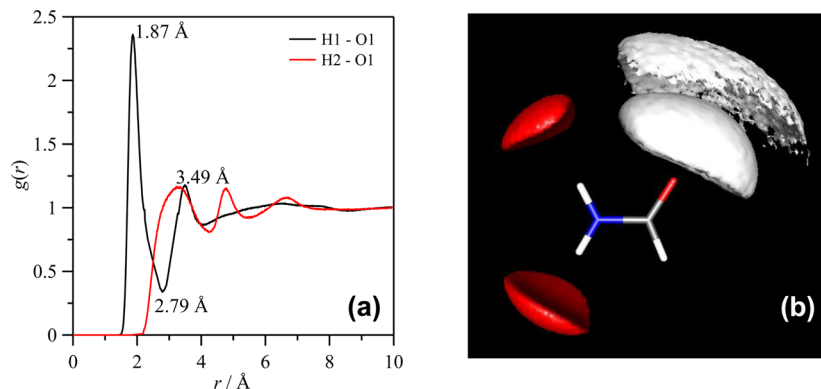


Figure 10. (a) Radial distribution functions, $g(r)$, and (b) spatial distribution functions for hydrogen atoms in FOR around FOR in pure FOR at 293 K. H1 and H2 stand for the $-\text{NH}_2$ and $-\text{COH}$ hydrogen atoms, respectively, and O1 stands for the $-\text{COH}$ oxygen atom. In panel b, white and red surfaces show H1 and O1 atoms, respectively. Spatial distribution functions are shown for isodensity values with 3 times bulk density.

Table 1. Number of Hydrogen Bonds, N_H , Calculated for Simulation Boxes Containing 500 Molecules in Pure Amides and Alkanediols at 293 K^a

	$H(\text{NH}_2)-\text{O}(\text{COH})$		$H(1)-\text{O}(1)$	$H(1)-\text{O}(2)$	$H(2)-\text{O}(2)$
FOR	412.2 ± 14.1	ED	192.6 ± 18.1	380.0 ± 12.3	198.4 ± 17.6
NMF	310.5 ± 11.1	PD	154.8 ± 15.9	330.9 ± 18.5	152.8 ± 18.2
		BD	199.9 ± 18.4	332.7 ± 12.1	139.6 ± 13.2

^aAll values calculated with 3.0 Å as the maximum hydrogen bond donor–acceptor distance and 50° as the maximum angle between the donor and acceptor. For pure amides, $H(\text{NH}_2)$ and $\text{O}(\text{COH})$ stand for H atoms in $-\text{NH}_2$ and O atoms in $-\text{COH}$ group; for pure alkanediols, H(1) and O(1) for H and O atoms in hydroxyl group in position 1 and H(2) and O(2) in position 2.

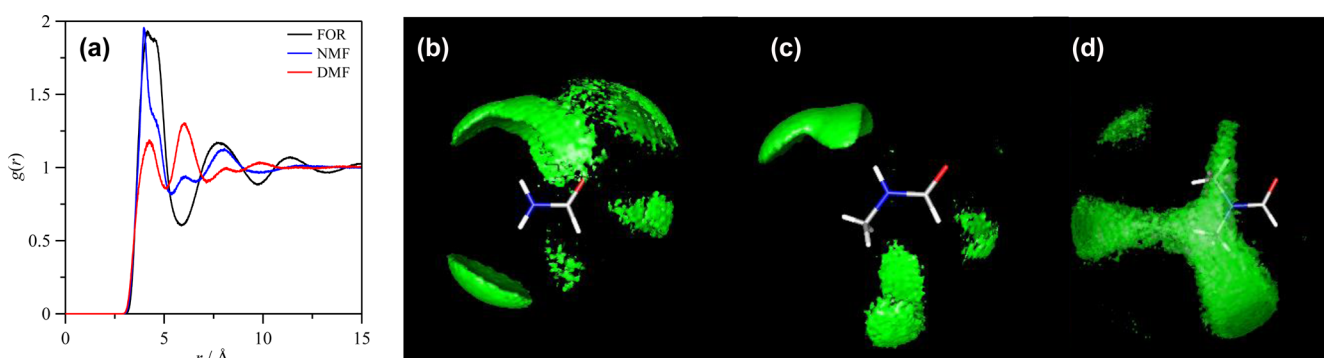


Figure 11. (a) Center-of-mass–center-of-mass radial distribution functions, $g(r)$, and (b–d) spatial distribution functions of the center of mass of amide molecules around a central amide, for pure amides at 293 K. Panels b–d show results for FOR, NMF, and DMF, respectively. Spatial distribution functions are shown for isodensity values with 3 times bulk density.

Molecular Dynamics Analysis. A detailed picture of the structuring and intermolecular interactions may be inferred from the classic molecular dynamics simulations carried out in this work. Considering that the main objective of this work is to analyze the intermolecular forces in the considered liquid systems, a brief analysis of the characteristics of pure formamides and alkanediols using the applied force field parametrization was carried out in the first place.

FOR molecules have two relevant hydrogen bond donor/acceptor sites as mentioned in previous sections: the $-\text{NH}_2$ and $-\text{COH}$ groups. In a first approach, it may be considered that hydrogen atoms belonging to both functional groups (H1 and H2) may develop H-bonds, but results reported in Figure 10a for radial distribution functions (RDFs) discard hydrogen atoms in the $-\text{COH}$ group (H2). Therefore, self-association in pure formamides is developed only through the interaction of hydrogen atoms in the $-\text{NH}_2$ group, as confirmed by spatial distribution functions (SDFs) in Figure 10b. Both hydrogen

atoms in the NH_2 group seem equivalent for H-bonding, and the solvation by hydrogen bonding around the oxygen atom in the COH group (O1) is developed through two well-defined solvation shells, Figure 10. The calculated number of H-bonds in pure FOR is reported in Table 1, which leads to roughly only 18% of the CO groups not H-bonded (slightly lower value than the one inferred from ATR-IR studies in Figure 5), showing the strong trend to self-aggregate for FOR molecules. The methylation of the NH_2 group leads to a weakening of H-bonding ability, which is completely absent in the case of DMF. RDFs for pure formamides are reported in Figure 11a. Comparison of FOR with NMF results shows that the first methylation of the amine group leads to the expected decrease of the number of H-bonds, Table 1, with 38% of non-H-bonded CO groups but also to a rearrangement of molecules. RDFs for centers of mass in Figure 11 show that the solvation structure around a central NMF molecule is very different from that in pure FOR, which is confirmed from SDF results in

Figure 11b and c. In the case of FOR molecules, neighbor molecules are highly concentrated around the CO group, whereas for NMF molecules are distributed around different spots and hindered around the methyl group. Likewise, in the case of DMF, in which intermolecular interactions are only developed through dipole–dipole interactions, it tends to concentrate around the amine group and thus avoids the head COH hydrogen bond acceptor site, Figure 11d.

It should be remarked that the number of H-bonds in pure formamides is strongly dependent on the criteria selected in the calculation; with reasonable donor–acceptor separation criteria (lower than 3.0 Å), the H-bond angle suffers remarkable changes with the used donor–acceptor angle, Figure 12.

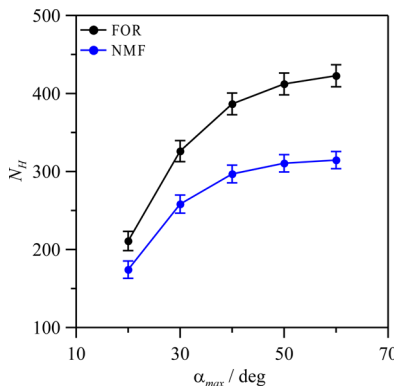


Figure 12. Number of hydrogen bonds, N_H , in pure FOR and NMF as a function of the maximum value of the hydrogen bond donor–acceptor angle, α_{\max} , at 293 K. Values calculated for a simulation box containing 500 amide molecules with 3.0 Å as the maximum donor–acceptor hydrogen bond distance.

Nevertheless, angles close to 50° may be considered as reasonable for the H-bonding definition, and thus, the interaction of neighbor FOR and NMF molecules is developed with donor–acceptor angles of 50° with lower populations of H-bonds in the 20–30° range, which may be justified considering the geometry of the NH_2 group in the formamide molecules.

Results reported in Figure 10 show that the interaction between neighbor formamide molecules is developed through two well-defined solvation shells around the CO group (especially for NMF) in which the H-bonding is developed. Therefore, the residence times of molecules inside this solvation region, composed by the first and second solvation spheres, were calculated to analyze the dynamics of solvation, Figure 13. These residence times should not be considered as a measure of the H-bond lifetimes (much shorter) because the size of the sphere considered for the calculation is larger than the 3.0 Å criteria used to define H-bonds. Results in Figure 13 show that molecules with stronger intermolecular interactions remain longer times around the CO atoms, and thus, the methylation of the amine group increases mobility around the CO H-bonding acceptor sites.

In the case of pure 1,2-alkanediols, the molecules contain two hydroxyl groups, which in a first approach could be considered as nonequivalent (for PD and BD) for H-bonding purposes. RDFs reported in Figure 14a split the different possible H-bonds as position 1–position 1, position 2–position 2, or position 1–position 2 (where position 1 and position 2 define hydroxyl groups in position 1 or 2). RDFs for these three

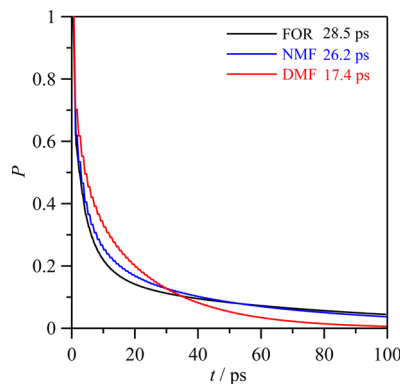


Figure 13. Exponential decay of conditional probability, P , for the center of mass of amide molecules to remain within a sphere of radius $R + \delta r$ around a given center of mass of another amide molecule, entering the sphere of radius $R - \delta r$ at time $t = 0$. P calculated for pure FOR, NMF, and DMF at 293 K. $R = 6.75$ Å, first solvation shell in Figure 11, and $\delta r = 0.25$ Å for the three amides. The residence time of the amide center of mass inside a sphere of radius R and centered in the amide center of mass was calculated from $P(t)$ and reported inside the panel.

possible interactions are analogous, with a first narrow peak showing strong H-bonding, which maxima in the case of BD appearing at 1.75, 1.79, and 1.83 Å for position 1–position 1, position 1–position 2, or position 2–position 2. Therefore, both hydroxyl groups are almost equivalent for all the studied formamides. Nevertheless, the calculated number of hydrogen bonds of type position 1–position 2 is remarkably larger than the two other options, Table 1. Therefore, H-bonding in pure alkanediols is mainly developed through H-bonding between the hydroxyl group in position 1 and position 2 but also maintaining relevant interactions through the other two options. Likewise, the average number of H-bonds per molecule is roughly 1.5 for the three studied alkanediols, and thus, the shape of the molecules hinders the development of two hydrogen bonds per molecule, leading to some free hydroxyl groups in the pure fluids. The high structuring around the hydroxyl groups may be inferred from the SDFs in Figure 14b and c, which show the spots corresponding to H-bonds around both hydroxyl groups, being equivalent in the case of ED and changing with methylation and ethylation. For PD, the solvation around the hydroxyl group is different from that around hydroxyl in position 2 because the presence of the methyl group hinders some regions around the hydroxyl group in position 2. This behavior is more evident for BD, Figure 14d, in which reinforcement around the hydroxyl group in position 1 is obtained when compared with ED, Figure 14b and d, and a shifting of solvation shells around the hydroxyl in position 2 is obtained. This is in agreement with the lower number of H-bonds for position 2–position 2 than for position 1–position 1 reported in Table 1 for BD, whereas for ED they are almost the same, and thus, position 2 may be considered as slightly hindered for H-bonding both for PD and BD.

The structuring and intermolecular hydrogen bonding should change remarkably when formamides and alkanediols are mixed because of the three functional groups which are able to act as H-bond donors and/or acceptors, with relative concentration varying with mixture mole fraction. RDFs reported in Figure 15a allow the two main H-bonds between FOR and ED molecules to be analyzed: (i) FOR acting as a H-bond donor, O(ED)–H(N, FOR), and (ii) ED acting as a H-

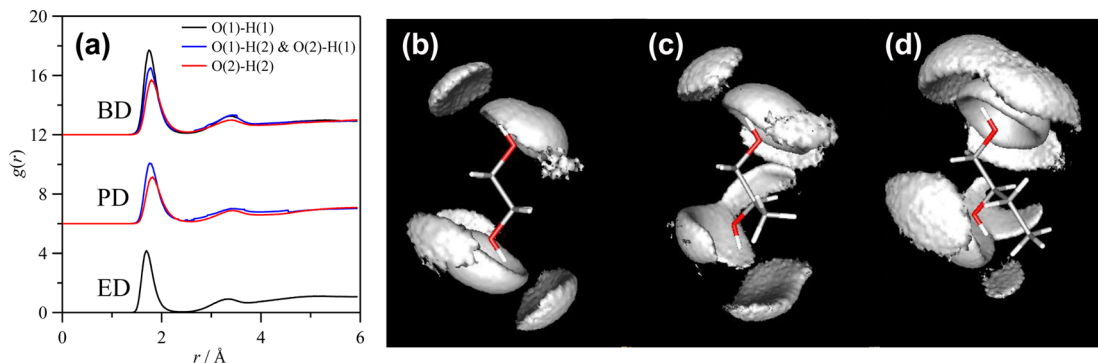


Figure 14. (a) Radial distribution functions, $g(r)$, and (b) spatial distribution functions, for hydrogen atoms in alkanediol around alkanediol in pure alkanediols at 293 K. $O(1)$ and $H(1)$ stand for atoms in the hydroxyl group in position 1, whereas $O(2)$ and $H(2)$, for those in position 2. Panels b–d show spatial distribution functions for both $H(1)$ and $H(2)$ atoms for isodensity values with 3 times bulk density.

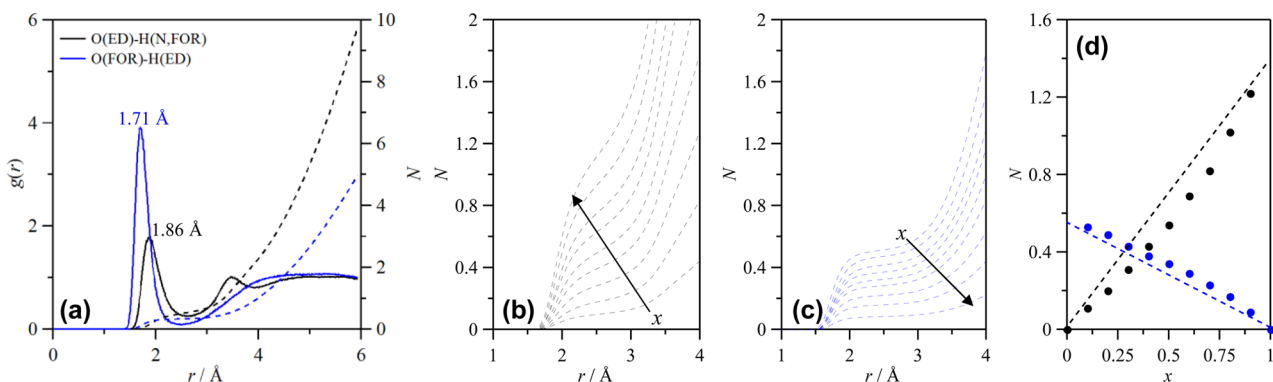


Figure 15. (a) Radial distribution functions, $g(r)$, and running integrals of $g(r)$, N , between oxygen and hydrogen atoms in ED ($O(ED)$) and H(ED), which correspond to H atoms in $-OH$ groups in positions 1 and 2) and FOR ($O(FOR)$) and H(FOR), which correspond to H atoms in the $-NH_2$ group), in the FOR + ED equimolar mixture at 293 K. Panels b and c show N for the same $g(r)$ as in panel a for x FOR + $(1 - x)$ ED, where x stands for mole fraction, at 293 K, with arrows showing increasing x starting from $x = 0.1$ to 0.9 in 0.1 steps. Panel d shows N values calculated up to the first minima in $g(r)$ shown in panel a, first solvation shell, for x FOR + $(1 - x)$ ED at 293 K.

bond acceptor, $O(FOR)-H(ED)$. Both RDFs are characterized by a first narrow and intense peak, with maxima at slightly larger distances for FOR acting as a donor and also weaker intensity for this peak. Therefore, although both types of H-bonding are possible, results in Figure 15a together with the corresponding running integrals reported in Figure 15b and c show a larger trend for ED acting as a H-bond donor. This is remarkable considering that both FOR and ED molecules have two hydrogen atoms which may lead to H-bonding. Likewise, the number of hydrogen atoms in the first solvation sphere obtained from the integration of RDFs in Figure 15a up to the first minima, those H-bonded, changes in a clearly nonlinear way with composition for oxygen atoms in both FOR and ED. Nevertheless, these deviations from the linear behavior show opposite trends; for oxygen atoms in ED, the number of hydrogen atoms around them is lower than the linear behavior, whereas, for oxygen atoms in FOR, it is larger, which confirms the larger trend of ED atoms to develop H-bonding with oxygen in FOR and the weaker opposite trend for hydrogen atoms in the FOR amine group with regard to oxygen atoms in ED. That is to say, hydroxyl affinity toward the CO group is larger than the amine affinity for hydroxyl groups.

The spatial arrangement around FOR and ED molecules in FOR + ED mixtures is reported for SDFs in Figure 16. The arrangement of FOR molecules around a central FOR molecule (homoassociations) follows similar patterns to those in pure FOR (Figures 11 and 16a) especially around the amine group.

Nevertheless, upon mixing with ED, the distribution of FOR molecules around another FOR changes for the region surrounding the COH group, the second solvation shell around the CO atom vanishes, and a new region of high density appears around the hydrogen atom in COH which was not present in pure FOR. These changes may be justified considering that results in Figure 16b show that ED occupy similar spatial regions around FOR molecules, and thus, considering the large affinity of hydroxyl atoms for the CO group in FOR, some FOR molecules will be shifted from their positions around the CO group toward the region beside the hydrogen atom in COH. Likewise, the development of FOR-ED interactions through hydrogen bonding around the ED hydroxyl groups, Figure 16c, also changes the distribution of ED molecules around another ED molecule, Figure 16d.

The strength of intermolecular forces developed in FOR + ED mixtures is analyzed in Figure 17, in which the total intermolecular energy (Coulombic plus Lennard-Jones) is split in FOR-FOR, ED-ED, and FOR-ED contributions. It should be remarked that FOR-ED heteroassociations are larger than any of the FOR-FOR or ED-ED homoassociations, which would justify the large deviations from ideality reported in Figure 2. These interaction energies follow an almost linear variation with composition for homoassociations, whereas for FOR-ED energies the behavior is clearly nonlinear with two well-defined regions separated by equimolar composition, which is in fair agreement with the change of thermophysical

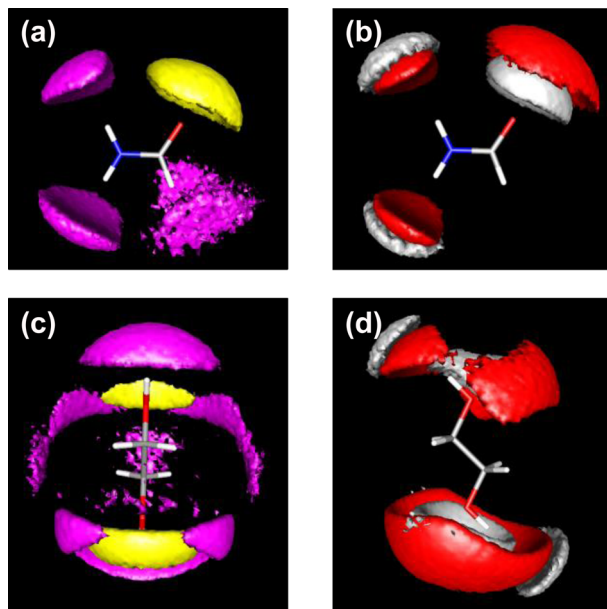


Figure 16. Spatial distribution functions in the FOR + ED equimolar mixture at 293 K for isodensity values with 3 times bulk density. Panels a and b show distributions around FOR molecules, and panels c and d, around ED molecules. Color code: (yellow) H atoms in the FOR $-NH_2$ group, (pink) O atoms in the FOR $-COH$ group, (gray) H atoms in the ED $-OH$ groups, and (red) O atoms in the ED $-OH$ groups.

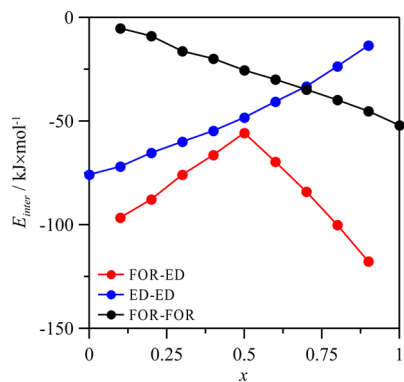


Figure 17. Total intermolecular interaction energy, E_{inter} (sum of Coulombic and Lennard-Jones contributions), in x FOR + $(1-x)$ ED mixtures at 293 K.

and spectroscopic properties reported in previous sections. Moreover, the total intermolecular interaction energy was split in Coulombic and Lennard-Jones contributions for all the studied systems, Table 2. In all the cases, the Coulombic term (purely electrostatic interaction) was larger than the Lennard-

Jones contribution. For ED containing mixtures, amide–alkanediol and alkanediol–alkanediol contributions change very slightly on going from FOR to DMF mixtures, which shows that the large ED affinity for the CO group in the amide is not remarkably affected by the methylation of the amide NH_2 group. Moreover, for FOR containing systems, the changes in all the intermolecular energy contributions do not change remarkably with increasing alkyl chain in 1,2-alkanediols; only the alkanediol–alkanediol Coulombic contribution decreases and the Lennard-Jones contribution increases with increasing alkyl chain. Nevertheless, the amide–alkanediol interaction energies do not change remarkably with increasing chain length in the alkanediol, confirming the large affinity of the alcohol for the amide CO group irrespective of the length of the alkyl chain.

The characteristics of the intermolecular interactions are also quantified through the number of H-bonds in the mixtures, Figure 18. For $x > 0.6$, FOR–FOR H-bonds are dominating in

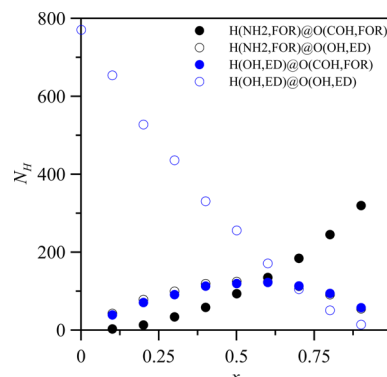


Figure 18. Number of hydrogen bonds, N_H , calculated for simulation boxes containing 500 total molecules in x FOR + $(1-x)$ ED mixtures at 293 K. Intermolecular hydrogen bonds were calculated between hydrogen atoms in the FOR $-NH_2$ group, $H(NH_2, \text{FOR})$, or hydrogen atoms in the ED $-OH$ group, $O(OH, \text{ED})$, and oxygen atoms in the FOR $-COH$ group, $O(COH, \text{FOR})$, or oxygen atoms in the ED $-OH$ group, $O(OH, \text{ED})$.

FOR–ED mixtures but they decrease in a linear way up to $x = 0.6$, whereas for lower compositions the decreasing rate follows a different trend. In the case of $x < 0.6$, ED–ED H-bonds dominate. The number of H-bonds corresponding to heteroassociations, FOR–ED, follows a pattern with a maximum at $x = 0.6$. Therefore, $x = 0.6$ is the composition at which the total number of H-bonds (homo- and heteroassociation) reaches the maximum value, including the maximum value for FOR–ED H-bonds, which would justify the highest nonidealality for mixtures around this composition. The effect of the amide and alkanediol type on H-bonds is

Table 2. Intermolecular Interaction Energy (Coulombic and Lennard-Jones Contributions) in Amide + ED and FOR + Alkanediol Equimolar Mixtures at 293 K

	amide–amide		amide–alkanediol		alkanediol–alkanediol	
	Coulombic	Lennard-Jones	Coulombic	Lennard-Jones	Coulombic	Lennard-Jones
FOR + ED	-19.2 ± 0.2	-6.3 ± 0.0	-43.5 ± 0.2	-12.3 ± 0.0	-45.0 ± 0.2	-3.4 ± 0.0
NMF + ED	-17.1 ± 0.1	-11.1 ± 0.0	-48.4 ± 0.2	-16.2 ± 0.0	-43.8 ± 0.2	-1.5 ± 0.0
DMF + ED	-8.7 ± 0.1	-15.6 ± 0.0	-41.0 ± 0.2	-19.7 ± 0.0	-44.2 ± 0.2	-0.5 ± 0.0
FOR + PD	-20.3 ± 0.2	-5.1 ± 0.0	-41.8 ± 0.2	-15.2 ± 0.0	-29.6 ± 0.2	-11.7 ± 0.0
FOR + BD	-19.3 ± 0.2	-4.3 ± 0.0	-43.2 ± 0.2	-16.5 ± 0.1	-32.2 ± 0.2	-15.2 ± 0.0

Table 3. Number of Hydrogen Bonds, N_H , Calculated for Simulation Boxes Containing 500 Total Molecules for Amide + Alkanediol Equimolar Mixtures at 293 K^a

	H(NH ₂)–O(COH)	H1(NH ₂)–O(1)&O(2)	H(1)&H(2)–O(COH)	H(1)&H(2)–O(1)&O(2)
FOR–ED	93.9	124.8	120.0	256.3
NMF–ED	64.0	76.7	143.4	242.2
DMF–ED			153.8	234.9
FOR–PD	95.0	102.3	127.7	178.2
FOR–BD	92.2	102.3	139.1	187.6

^aAll values calculated with 3.0 Å as the maximum hydrogen bond donor–acceptor distance and 50° as the maximum angle between the donor and acceptor. H(NH₂) and O(COH) stand for H atoms in –NH₂ and O atoms in the –COH group of amide molecules; H(1) and O(1) for H and O atoms in hydroxyl group in position 1, and H(2) and O(2) in position 2, of alkanediol molecules.

summarized in Table 3. In the case of FOR containing systems, H-bonds corresponding to FOR–alkanediol interactions suffer a very minor decrease with increasing alkyl change in the alkanediol, and also a larger decrease in the number of alkanediol–alkanediol interactions, in agreement with interaction energies in Table 2. For systems containing ED, the effect of methylation in the amide decreases the number of alkanediol–alkanediol interactions but increases the number of amide–ED H-bonds because of the larger Lennard-Jones contributions reported in Table 2.

The residence times for atoms involved in homo- and heteroassociation through H-bonding in FOR + ED mixtures as a function of composition are reported in Figure 19. Residence

times for interactions involving ED molecules are remarkably large, both for alkanediol–alkanediol homoassociations and alkanediol–FOR heteroassociations, in fair agreement with the interaction strengths reported in Table 2. Al residence times decrease with increasing FOR mole fraction in a linear way. The largest values are obtained for FOR–ED heteroassociations in which FOR acts as a H-bond acceptor, whereas FOR–ED interactions with FOR acting as H-bond donors lead to residence times less than the half, showing the strong tendency of the CO group for acting as a donor. For FOR mixtures, residence times around the FOR molecule suffer slight increases with increasing alkyl chain in the alkanediol, whereas for ED containing mixtures all the residence times increase remarkably with amide methylation. For example, residence times for hydrogen atoms in the ED hydroxyl group around the CO amide group are roughly 3 times larger for DMF than for FOR containing mixtures, Table 4.

To recap the main issues in the studied mixtures, the center-of-mass RDFs are reported in Figure 20, showing the effect of

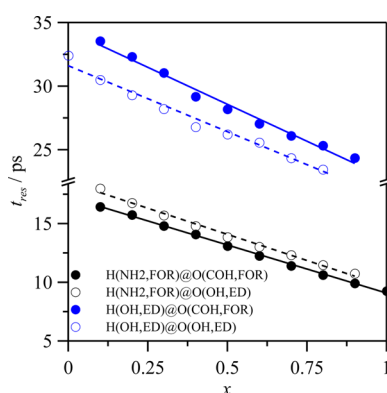


Figure 19. Residence time, t_{res} , of hydrogen atoms in the FOR –NH₂ group, H(NH₂, FOR), or hydrogen atoms in the ED –OH group, H(OH, ED), around oxygen atoms in the FOR –COH group, O(COH, FOR), or around oxygen atoms in the ED –OH group, O(OH, ED), in x FOR + (1 – x) ED mixtures at 293 K. t_{res} was calculated from the exponential decay of conditional probability P as in Figure 13 with $R = 3.0$ Å.

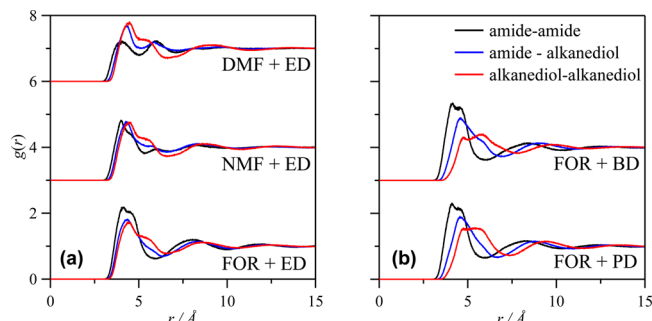


Figure 20. Radial distribution functions, $g(r)$, between the center of mass of involved molecules in amide + alkanediol equimolar mixtures at 293 K.

Table 4. Residence Time, t_{res} (ps), of Hydrogen Atoms in the Amide –NH₂ Group, H(NH₂), or Hydrogen Atoms in the Alkanediol –OH Group, H(1) and H(2) (for Hydroxyl Groups in Positions 1 and 2, Respectively), around Oxygen Atoms in the Amide –COH Group, O(COH), or around Oxygen Atoms in the Alkanediol –OH Group, O(1) and O(2) (for Hydroxyl Groups in Positions 1 and 2, Respectively), in Amide + Alkanediol Equimolar Mixtures at 293 K^a

	H(NH ₂)@O(COH)	H1(NH ₂)@O(1)&O(2)	H(1)&H(2)@O(COH)	H(1)&H(2)@O(1)&O(2)
FOR–ED	13.1	13.86	28.19	26.21
NMF–ED	19.7	19.41	53.29	33.43
DMF–ED			74.01	35.49
FOR–PD	13.03	12.63	26.57	22.17
FOR–BD	15.55	15.73	35.12	29.16

^a t_{res} was calculated from the exponential decay of conditional probability P as in Figure 13 with $R = 3.0$ Å.

amide and alkanediol type involved in the mixture. For a selected 1,2-alkanediol, ED in Figure 20a, only amide–amide RDFs suffer remarkable changes with amide methylation, because of the weakening of amide–amide H-bonding, whereas the structuring for amide–alkanediol and alkanediol–alkanediol interactions is not remarkably affected by the type of considered amide. For the effect of alkanediol, Figure 20b, very weak structural changes are inferred for all the homo- and heteroassociations, confirming the possibility of developing amide–alkanediol very efficient H-bonding irrespective of the length of the alkyl chain in the 1,2-alkanediol. Finally, the effect of temperature on intermolecular interactions in the 283–313 K range is summarized in Figure 21. All the involved

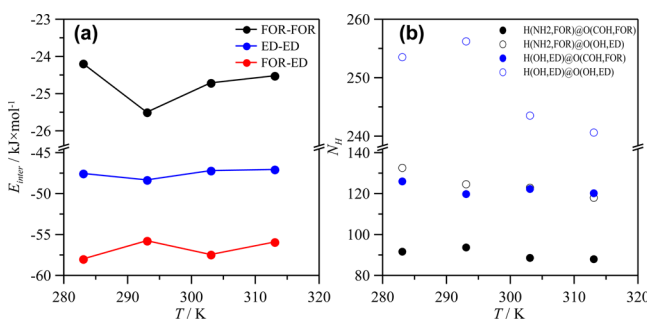


Figure 21. (a) Total intermolecular interaction energy, E_{inter} (sum of Coulombic and Lennard-Jones contributions), and (b) number of hydrogen bonds, N_H , calculated for simulation boxes containing 500 total molecules, in FOR + ED equimolar mixtures as a function of temperature.

intermolecular forces are strong enough to remain almost without changes in the studied temperature range, intermolecular interaction energy, Figure 21a, and the number of H-bonds, Figure 21b, remains almost constant. The number of H-bonds decreases roughly 6% for all the possible interacting pairs. Therefore, the changes in excess and mixing properties with temperature reported in Figure 2 should be considered as a result of expansions with increasing temperature which lead to minor changes in intermolecular interactions.

CONCLUSIONS

The structure, properties, and intermolecular interactions in formamides (FOR, NMF, or DMF) + 1,2-alkanediols (ED, PD, or BD) are studied using a combined experimental and theoretical approach. The used methodology allows the macro- and nanoscopic characteristics of these relevant systems and the connections between them to be analyzed. The characteristics of these fluids are mainly controlled by the strong trend to develop H-bonding because of the three involved functional groups that may act as H-bond donors and/or acceptors. Hydroxyl groups in alkanediols show a large affinity for amide carbonyl groups, and thus, very efficient H-bonding is developed through these positions. The properties of the mixtures are largely nonideal, which from a nanoscopic viewpoint is justified considering the existence of two well-defined regions as a function of mixture composition, those with amide molar fraction larger than 0.6 in which the amide–amide interactions prevail, and those with lower mole fractions in which the amide–alkanediol interactions are optimal and combined with strong alkanediol–alkanediol interactions. The large affinity between amides and alkanediol molecules is not remarkably changed neither by the amide methylation nor by

the increase in the alkyl chain of the alkanediol, and remains almost constant in the studied temperature range.

ASSOCIATED CONTENT

Supporting Information

Table S1 (physicochemical properties of pure compounds), Table S2 (force field parametrization), Tables S3–S5 (physicochemical properties of amide + 1,2-alkanediols), Table S6 (solvatochromic data), and Figures S1–S14 (DFT results on formamide + 1,2-alkanediol clusters). This material is available free of charge via the Internet at <http://pubs.acs.org>.

AUTHOR INFORMATION

Corresponding Authors

*E-mail: jose.trenzado@ulpgc.es.

*E-mail: sapar@ubu.es.

Notes

The authors declare no competing financial interest.

ACKNOWLEDGMENTS

This work was made possible by Ministerio de Economía y Competitividad (Spain, project CTQ2013-40476-R) and Junta de Castilla y León (Spain, project BU324U14). G.G. acknowledges the funding by Junta de Castilla y León, cofunded by European Social Fund, for a postdoctoral contract. We also acknowledge The Foundation of Supercomputing Center of Castile and León (FCSCL, Spain), Computing and Advanced Technologies Foundation of Extremadura (CénitS, LUSITANIA Supercomputer, Spain), and Consortium of Scientific and Academic Services of Cataluña (CSUC, Spain) for providing supercomputing facilities. The statements made herein are solely the responsibility of the authors.

REFERENCES

- Gray, C. G.; Gubbins, K. E.; Joslin, C. G. *Theory of Molecular Fluids. Applications*; Oxford University Press: London, 2011.
- Israelachvili, J. N. *Intermolecular and Surface Properties*; Academic Press: Oxford, U.K., 2011.
- Hansen, J. P.; McDonald, I. R. *Theory of Simple Liquids with Applications to Soft Matter*; Academic Press: Oxford, U.K., 2013.
- Reichardt, C.; Welton, T. *Solvents and Solvent Effects in Organic Chemistry*; Wiley-VCH: Weinheim, Germany, 2011.
- de With, G. *Liquid-State Physical Chemistry. Fundamentals, Modelling, and Applications*; Wiley-VCH: Weinheim, Germany, 2013.
- Goerigk, L.; Grimme, S. A Thorough Benchmark of Density Functional Methods for General Main Group Thermochemistry, Kinetics, and Noncovalent Interactions. *Phys. Chem. Chem. Phys.* **2011**, *13*, 6670–6688.
- Israelachvili, J.; Ruths, M. Brief History of Intermolecular and Intersurface Forces in Complex Fluid Systems. *Langmuir* **2013**, *29*, 9605–9619.
- Hands, M. D.; Slipchenko, L. V. Intermolecular Interactions in Complex Liquids: Effective Fragment Potential Investigation of Water-tet-Butanol Mixtures. *J. Phys. Chem. B* **2012**, *116*, 2775–2786.
- García, J. I.; García-Marín, H.; Mayoral, J. A.; Pérez, P. Quantitative Structure-Property Relationships Prediction of Some Physico-Chemical Properties of Glycerol Based Solvents. *Green Chem.* **2013**, *15*, 2283–2293.
- Lane, J. S.; Richens, J. L.; Vere, K. A.; O’Shea, P. Rational Targeting of Subclasses of Intermolecular Interactions: Elimination of Nonspecific Binding for Analyte Sensing. *Langmuir* **2014**, *30*, 9457–6465.
- Kobko, N.; Paraskevas, L.; del Rio, E.; Dannenberg, J. J. Cooperativity in Amide Hydrogen Bonding Chains: Implications for Protein-Folding Models. *J. Am. Chem. Soc.* **2001**, *123*, 4348–4349.

- (12) Tsuchida, E. Ab Initio Molecular-Dynamics Study of Liquid Formamide. *J. Chem. Phys.* **2004**, *121*, 4740–4746.
- (13) Chebaane, A.; Hammami, F.; Bahri, M.; Nasr, S. Intramolecular and Intermolecular Interactions on N-methylformamide - Water Mixture: X-ray Scattering and DFT calculation Study. *J. Mol. Liq.* **2012**, *165*, 133–138.
- (14) Wang, Y.; Guo, M.; Wei, S.; Yin, S.; Wang, Y.; Song, Z.; Hofmann, M. R. Intermolecular Hydrogen Bonding of N-Methyl-formamide in Aqueous Environment: A Theoretical Study. *Comput. Theor. Chem.* **2014**, *1049*, 28–34.
- (15) Stalylowicz, H.; Krygowski, T. M.; Palusiak, M. Modeling the Electronic Structure of Formamide: an Acid/Base Amphoteric Solvent. *Struct. Chem.* **2012**, *23*, 1711–1721.
- (16) Moity, L.; Durand, M.; Benazzouz, A.; Pierlot, C.; Molinier, V.; Aubry, J. M. Panorama of Sustainable Solvents Using the COSMO-RS Approach. *Green Chem.* **2012**, *14*, 1132–1145.
- (17) Pathak, P. N. N,N-dialkylamides as Extractants for Spent Fuel Reprocessing: An Overview. *J. Radioanal. Nucl. Chem.* **2014**, *300*, 7–15.
- (18) Azofra, L. M.; Altarsa, M.; Ruiz-lópez, M. F.; Ingrosso, F. A Theoretical Investigation of the CO₂-philicity of amides and carbamides. *Theor. Chem. Acc.* **2013**, *132*, 1326.
- (19) Shokouhi, M.; Farahani, H.; Hosseini-Jenab, M. Experimental Solubility of Hydrogen Sulfide and Carbon Dioxide in Dimethylformamide and Dimethylsulfoxide. *Fluid Phase Equilib.* **2014**, *367*, 29–37.
- (20) Saladino, R.; Crestini, C.; Pino, S.; Costanzo, G.; Di Mauro, E. Formamide and the Origin of Life. *Phys. Life Rev.* **2012**, *9*, 84–104.
- (21) Jadzyn, J.; Swiergiel, J. On Similarity of Hydrogen-Bonded Networks in Liquid Formamide and Water as Revealed in the Static Dielectric Studies. *Phys. Chem. Chem. Phys.* **2012**, *14*, 3170–3175.
- (22) Bakó, I.; Megydes, T.; Bálint, S.; Chihaiia, V.; Bellissent-Funel, M. C.; Krienke, H.; Kopf, A.; Suh, S. H. Hydrogen Bonded Network Properties in Liquid Formamide. *J. Chem. Phys.* **2010**, *132*, 014506.
- (23) Biswas, S.; Mallik, B. Effects of Temperature on the Structure and Dynamics of Aqueous Mixtures of N,N-Dimethylformamide. *J. Chem. Eng. Data* **2014**, *59*, 3250–3257.
- (24) Cordeiro, J. M.M.; Soper, A. K. Neutron Diffraction Stdy on Liquid N-Methylformamide using EPSR Simulation. *J. Phys. Chem. B* **2009**, *113*, 6819–6825.
- (25) Chalarich, M.; Samios, J. Systematic Molecular Dynamics Studies of Liquid N,N-Dimethylformamide Using Optimized Rigid Forcefields: Investigation of the Thermodynamic, Structural, Transport and Dynamic Properties. *J. Chem. Phys.* **2000**, *112*, 8581–8594.
- (26) Lei, Y.; Li, H.; Pan, H.; Han, S. Structures and Hydrogen Bonding Analysis of N,N-Dimethylformamide and N,N-dimethylformamide - Water Mixtures by Moleular Dynamics Simulations. *J. Phys. Chem. B* **2003**, *107*, 1574–1583.
- (27) Okada, M.; Ibuki, K.; Ueno, M. Temperature Effect on the Reorientational Correlation Time of Water in Formamide- and N,N-Dimethylformamide-Water mixtures. *Bull. Chem. Soc. Jpn.* **2012**, *85*, 189–200.
- (28) Feng, W.; Jia, G. Z. The Hydrogen Bonding Dynamics and Cooperative Interactions in Aqueous N,N-Dimethylformamide Solution Studied by Dielectric Relaxation Spectroscopy. *Physica A* **2014**, *404*, 315–322.
- (29) Rani, M.; Maken, S. Topological Studies of Molecular Interactions of Formamide with Propanol and Butanol at 298.15 K. *J. Ind. Eng. Chem.* **2012**, *18*, 1694–1704.
- (30) Rani, M.; Gahlyan, S.; Gaur, A.; Maken, S. Ultrasonic Study on Molecular Interactions in Binary Mixtures of Formamide with 1-Propanol or 2-Propanol. *Chin. J. Chem. Eng.* **2014**, DOI: 10.1016/j.cjche.2014.12.003.
- (31) Sengwa, R. J.; Choudhary, S.; Bald, A. Dielectric Dispersion and Electric Relaxation Processes Induced by Ionic Conduction in Formamide, 2-aminoethanol and Their Binary Mixtures. *J. Solution Chem.* **2013**, *42*, 1960–1975.
- (32) Sengwa, R. J.; Choudhary, S.; Khatri, V. Characterization of Dominant Hydrogen Bonded Complex Structures of Dielectroc Polarisation and Viscous Flow Processes in Glycerol-Formamide Binary Mixtures. *J. Solution Chem.* **2011**, *40*, 154–163.
- (33) Weng, L.; Chen, C.; Zuo, J.; Li, W. Molecular Dynamics Study of Effects of Temperature and Concentration on Hydrogen-Bond Abilities of Ethylene Glycol and Glycerol: Implications for Cryopreservation. *J. Phys. Chem. A* **2011**, *115*, 4729–4737.
- (34) Kaiser, A.; ismailova, O.; Koskela, A.; Huber, S. E.; Ritter, M.; Cosenza, B.; Bneger, W.; Nazmutdinov, R.; Probst, M. Ethylene Glycol Revisited: Moleuclar Dynamics Simulations and Visualization of the Liquid and Its Hydrogen-Bond Network. *J. Mol. Liq.* **2014**, *189*, 20–29.
- (35) Kulszewski, T.; Pleiss, J. A Molecular Dynamics Study of Liquid Aliphatic Alcohols: Simulation of Density and Self-Diffusion Coefficient Using a Modified OPLS Force Field. *Mol. Simul.* **2013**, *39*, 754–767.
- (36) García, G.; Trenzado, J. L.; Alcalde, R.; Rodríguez-Delgado, A.; Atilhan, M.; Aparicio, S. Structure of Alkylcarbonate + n-Alkane Mixed Fluids. *J. Phys. Chem. B* **2014**, *116*, 11310–11322.
- (37) Aparicio, S.; Davila, M. J.; Alcalde, R. Insights into the Coal Extractive Solvent N-Methyl-2-pyrrolidone + Carbon Disulfide. *Energy Fuels* **2009**, *23*, 1591–1602.
- (38) Reichardt, C. Solvatochromic Dyes as Solvent Polarity Indicators. *Chem. Rev.* **1994**, *94*, 2319–2358.
- (39) García, B.; Aparicio, S.; Alcalde, R.; Ruiz, R.; Dávila, M. J.; Leal, J. M. Characterization of Lactam - Containing Binary Solvents by Siolvatochromic Indicators. *J. Phys. Chem. B* **2004**, *108*, 3024–3029.
- (40) Becke, A. D. Density-Functional Exchange-Energy Approximation with Correct Asymptotic Behavior. *Phys. Rev. A* **1988**, *38*, 3098–3100.
- (41) Lee, C.; Yang, W.; Parr, R. G. Development of the Colle-Salvetti Correlation-Energy Formula into a Functional of the Electron Density. *Phys. Rev. B* **1988**, *37*, 785–789.
- (42) Becke, A. D. Density-Functional Thermochemistry. III. The Role of Exact Exchange. *J. Chem. Phys.* **1993**, *98*, 5648–5652.
- (43) Simon, S.; Duran, M.; Dannenberg, J. J. How Does Basis Set Superposition Error Change the Potential Surfaces for Hhydrogen-Bonded Dimers? *Chem. Phys.* **1996**, *105*, 11024–11031.
- (44) Frisch, M. J.; Trucks, G. W.; Schlegel, H. B.; Scuseria, G. E.; Robb, M. A.; Cheeseman, J. R.; Scalmani, G.; Barone, V.; Mennucci, B.; Petersson, G. A.; et al. *Gaussian 09*, revision D.01; Gaussian, Inc.: Wallingford, CT, 2010.
- (45) Lyubartsev, A. P.; Laaksonen, A. MDynaMix - A Scalable Portable Parallel MD Simulation Package for Arbitrary Molecular Mixtures. *Comput. Phys. Commun.* **2000**, *128*, 565–589.
- (46) Martínez, L.; Andrade, R.; Birgin, E. G.; Martínez, J. M. Packmol: A Package for Building Initial Configurations for Molecular Dynamics Simulations. *J. Comput. Chem.* **2009**, *30*, 2157–2164.
- (47) Essmann, U. L.; Perera, M. L.; Berkowitz, T.; Darden, H.; Lee, H.; Pedersen, L. G. A Smooth Particle Mesh Ewald Method. *J. Chem. Phys.* **1995**, *103*, 8577–8593.
- (48) Tuckerman, M.; Berne, B. J.; Martyna, G. J. Reversible Multiple Time Scale Molecular Dynamics. *J. Chem. Phys.* **1992**, *97*, 1990–2001.
- (49) Fumino, K.; Fossog, V.; Wittler, K.; Hempelmann, R.; Ludwig, R. Dissecting the Interaction Energy Between Anions and Cations in Protic Ionic Liquids. *Angew. Chem., Int. Ed.* **2013**, *52*, 2368–2352.